

High-Statistics Measurement of Collins and Sivers Asymmetries for Transversely Polarized Deuterons

G. D. Alexeev²⁸ M. G. Alexeev^{20,19} C. Alice^{20,19} A. Amoroso^{20,19} V. Andrieux³³ V. Anosov²⁸ S. Asatryan¹
 K. Augsten⁴ W. Augustyniak²³ C. D. R. Azevedo²⁶ B. Badelek²⁵ J. Barth⁸ R. Beck⁸ J. Beckers¹² Y. Bedfer⁶
 J. Bernhard³⁰ M. Bodlak⁵ F. Bradamante¹⁷ A. Bressan^{18,17} W.-C. Chang³¹ C. Chatterjee¹⁷ M. Chiosso^{20,19}
 A. G. Chumakov²⁹ S.-U. Chung^{12,††,§§} A. Cicuttin^{17,16} P. M. M. Correia²⁶ M. L. Crespo^{17,16} D. D'Ago^{18,17}
 S. Dalla Torre¹⁷ S. S. Dasgupta¹⁴ S. Dasgupta^{17,||} F. Delcarro^{20,19} I. Denisenko²⁸ O. Yu. Denisov¹⁹
 S. V. Donskov²⁹ N. Doshita²² Ch. Dreisbach¹² W. Dünnweber¹³ R. R. Dusaev²⁹ D. Ecker¹² D. Eremeev²⁹
 P. Faccioli²⁷ M. Faessler¹³ M. Finger⁵ M. Finger, Jr.¹⁰ H. Fischer¹⁰ K. J. Flöhner⁸ W. Florian^{17,16}
 J. M. Friedrich¹² V. Frolov²⁸ L. G. Garcia Ordóñez^{17,16} F. Gautheron^{17,33} O. P. Gavrichtchouk²⁸
 S. Gerassimov^{29,12} J. Giarra¹¹ D. Giordano^{20,19} A. Grasso^{20,19} A. Gridin²⁸ M. Grosse Perdekamp³³
 B. Grube¹² M. Grüner⁸ A. Guskov²⁸ P. Haas¹² D. von Harrach¹¹ M. Hoffmann⁸ A. Hohmrtsyan¹
 N. d'Hose⁶ C.-Y. Hsieh³¹ S. Huber¹² S. Ishimoto^{22,††} A. Ivanov²⁸ T. Iwata²² V. Jary⁴ R. Joosten⁸
 E. Kabuš¹¹ F. Kaspar¹² A. Kerbizi^{18,17} B. Ketzer⁸ A. Khatun⁶ G. V. Khaustov²⁹ T. Klasek⁵ F. Klein⁹
 J. H. Koivuniemi^{7,33} V. N. Kolosov²⁹ K. Kondo Horikawa²² I. Konorov^{29,12} V. F. Konstantinov^{29,†}
 A. Yu. Korzenev²⁸ A. M. Kotzinian^{1,19} O. M. Kouznetsov²⁸ A. Koval²³ Z. Kral⁵ F. Krinner¹² F. Kunne⁶
 K. Kurek²³ R. P. Kurjata²⁴ A. Kveton¹⁵ K. Lavickova⁴ S. Levorato¹⁷ Y.-S. Lian^{31,¶¶} J. Lichtenstadt¹⁵
 P.-J. Lin³² R. Longo³³ V. E. Lyubovitskij^{29,§} A. Maggiora¹⁹ A. Magnon^{14,†} N. Makke¹⁷ G. K. Mallot^{30,10}
 A. Maltsev²⁸ A. Martin^{18,17,*} J. Marzec²⁴ J. Matoušek⁵ T. Matsuda²¹ G. Mattson³³ C. Menezes Pires²⁷
 F. Metzger⁸ M. Meyer^{33,6} W. Meyer⁷ Yu. V. Mikhailov^{29,†} M. Mikhaseko^{13,‡} E. Mitrofanov²⁸ D. Miura²²
 Y. Miyachi²² R. Molina^{17,16} A. Moretti^{18,17} A. Movsisyan¹ A. Nagaytsev²⁸ D. Neyret⁶ M. Niemiec²⁵
 J. Nový⁴ W.-D. Nowak¹¹ G. Nukazuka²² A. G. Olshevsky²⁸ M. Ostrick¹¹ D. Panzieri^{19,¶¶}
 B. Parsamyan^{1,19,30,*} S. Paul¹² H. Pekeler⁸ J.-C. Peng³³ M. Pešek⁵ D. V. Peshekhonov²⁸ M. Pešková⁵
 S. Platchkov⁶ J. Pochodzalla¹¹ V. A. Polyakov²⁹ M. Quaresma²⁷ C. Quintans²⁷ G. Reicherz⁷ C. Riedl³³
 D. I. Ryabchikov^{29,12} A. Rychter²⁴ A. Rymbekova²⁸ V. D. Samoylenko²⁹ A. Sandacz²³ S. Sarkar¹⁴
 I. A. Savin^{28,†} G. Sbrizzai¹⁷ H. Schmieden⁹ A. Selyunin²⁸ K. Sharko²⁹ L. Sinha¹⁴ D. Spülbeck⁸ A. Srnka²
 M. Stolarski²⁷ M. Sulc³ H. Suzuki^{22,***} Y. Takanashi²² S. Tessaro¹⁷ F. Tessarotto^{17,*} A. Thiel⁸ F. Tosello¹⁹
 A. Townsend^{33,||} T. Triloki¹⁷ V. Tskhay²⁹ B. Valinoti^{17,16} B. M. Veit¹¹ J. F. C. A. Veloso²⁶ B. Ventura⁶
 A. Vijayakumar³³ M. Virius⁴ M. Wagner⁸ S. Wallner¹² K. Zaremba²⁴ M. Zavertyaev²⁹ M. Zemko^{5,4}
 E. Zemlyanichkina²⁸ and M. Ziembicki²⁴

(COMPASS Collaboration)

¹A.I. Alikhanyan National Science Laboratory, 2 Alikhanyan Br. Street, 0036, Yerevan, Armenia

²Institute of Scientific Instruments of the CAS, 61264 Brno, Czech Republic

³Technical University in Liberec, 46117 Liberec, Czech Republic

⁴Czech Technical University in Prague, 16636 Prague, Czech Republic

⁵Charles University, Faculty of Mathematics and Physics, 12116 Prague, Czech Republic

⁶IRFU, CEA, Université Paris-Saclay, 91191 Gif-sur-Yvette, France

⁷Universität Bochum, Institut für Experimentalphysik, 44780 Bochum, Germany

⁸Universität Bonn, Helmholtz-Institut für Strahlen- und Kernphysik, 53115 Bonn, Germany

⁹Universität Bonn, Physikalisches Institut, 53115 Bonn, Germany

¹⁰Universität Freiburg, Physikalisches Institut, 79104 Freiburg, Germany

¹¹Universität Mainz, Institut für Kernphysik, 55099 Mainz, Germany

¹²Technische Universität München, Physik Dept., 85748 Garching, Germany

¹³Ludwig-Maximilians-Universität, 80539 München, Germany

¹⁴Matrivani Institute of Experimental Research & Education, Calcutta-700 030, India

¹⁵Tel Aviv University, School of Physics and Astronomy, 69978 Tel Aviv, Israel

¹⁶Abdus Salam ICTP, 34151 Trieste, Italy

¹⁷Trieste Section of INFN, 34127 Trieste, Italy

¹⁸University of Trieste, Dept. of Physics, 34127 Trieste, Italy

¹⁹*Torino Section of INFN, 10125 Torino, Italy*²⁰*University of Torino, Dept. of Physics, 10125 Torino, Italy*²¹*University of Miyazaki, Miyazaki 889-2192, Japan*²²*Yamagata University, Yamagata 992-8510, Japan*²³*National Centre for Nuclear Research, 02-093 Warsaw, Poland*²⁴*Warsaw University of Technology, Institute of Radioelectronics, 00-665 Warsaw, Poland*²⁵*University of Warsaw, Faculty of Physics, 02-093 Warsaw, Poland*²⁶*University of Aveiro, 3810-193 Aveiro, Portugal*²⁷*LIP, 1649-003 Lisbon, Portugal*²⁸*Affiliated with an international laboratory covered by a cooperation agreement with CERN*²⁹*Affiliated with an institute covered by a cooperation agreement with CERN*³⁰*CERN, 1211 Geneva 23, Switzerland*³¹*Academia Sinica, Institute of Physics, Taipei 11529, Taiwan*³²*Center for High Energy and High Field Physics and Dept. of Physics, National Central University, 300 Zhongda Rd., Zhongli 320317, Taiwan*³³*University of Illinois at Urbana-Champaign, Dept. of Physics, Urbana, Illinois 61801-3080, USA*

(Received 30 December 2023; revised 22 March 2024; accepted 8 May 2024; published 5 September 2024)

New results are presented on a high-statistics measurement of Collins and Sivers asymmetries of charged hadrons produced in deep inelastic scattering of muons on a transversely polarized ${}^6\text{LiD}$ target. The data were taken in 2022 with the COMPASS spectrometer using the 160 GeV muon beam at CERN, statistically balancing the existing data on transversely polarized proton targets. The first results from about two-thirds of the new data have total uncertainties smaller by up to a factor of three compared to the previous deuteron measurements. Using all the COMPASS proton and deuteron results, both the transversity and the Sivers distribution functions of the u and d quark, as well as the tensor charge in the measured x range are extracted. In particular, the accuracy of the d quark results is significantly improved.

DOI: 10.1103/PhysRevLett.133.101903

^{*}Corresponding author.

[†]Deceased.

[‡]Also at ORIGINS Excellence Cluster, 85748 Garching, Germany.

[§]Also at Institut für Theoretische Physik, Universität Tübingen, 72076 Tübingen, Germany.

^{||}Present address: NISER, Centre for Medical and Radiation Physics, Bhubaneswar, India.

[¶]Also at University of Eastern Piedmont, 15100 Alessandria, Italy.

^{**}Also at Chubu University, Kasugai, Aichi 487-8501, Japan.

^{††}Also at KEK, 1-1 Oho, Tsukuba, Ibaraki 305-0801, Japan.

^{‡‡}Also at Department of Physics, Pusan National University, Busan 609-735, Republic of Korea.

^{§§}Also at Physics Department, Brookhaven National Laboratory, Upton, New York 11973, USA.

^{|||}Also at Department of Natural Sciences, Fairmont State University, 1201 Locust Ave, Fairmont, West Virginia 26554, USA.

^{¶¶}Also at Department of Physics, National Kaohsiung Normal University, Kaohsiung County 824, Taiwan.

Published by the American Physical Society under the terms of the [Creative Commons Attribution 4.0 International license](#). Further distribution of this work must maintain attribution to the author(s) and the published article's title, journal citation, and DOI. Funded by SCOAP³.

Transverse spin effects observed several decades ago in high-energy hadron-hadron interactions [1] originally constituted a challenge to quantum chromodynamics (QCD) [2]. Intense theoretical work [3–5] followed, and pioneering results were produced by the HERMES [6,7] and COMPASS [8–10] Collaborations in semi-inclusive hadron production measurements of deep inelastic lepton-nucleon scattering (SIDIS) off transversely polarized proton and deuteron targets. The current theoretical description [11] involves both the longitudinal and intrinsic transverse motion of partons inside a hadron, and the spin degrees of freedom. In this scheme, the description of a polarized nucleon within the leading-twist approximation of perturbative QCD requires eight transverse-momentum-dependent (TMD) parton distribution functions (PDFs), which describe the distributions of longitudinal and transverse momenta of partons and their correlations with nucleon and quark spins. Of particular interest in this 3D description of the nucleon are two of these PDFs, the transversity function h_1^q and the Sivers function $f_{1T}^{\perp q}$.

For a given quark flavor q , h_1^q is the analog of the helicity distribution g_1^q in the case of transversely polarized nucleons [3], i.e., the difference of the number of quarks with spin parallel to the nucleon spin and the number of quarks with spin opposite to the nucleon spin in transversely polarized nucleons. Together with g_1^q and the number

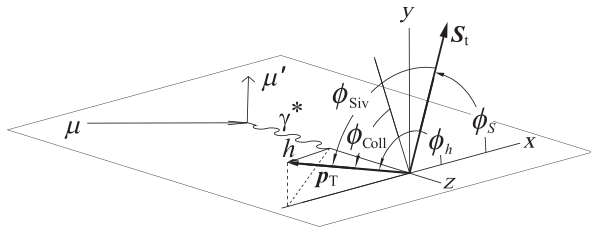


FIG. 1. The SIDIS reference system defined according to Ref. [22] and definition of the azimuthal angles. Here S_t and p_T are the projections of the quark spin vector and of the hadron h momentum vector, respectively, onto the plane transverse to the direction of the virtual photon γ^* .

density f_1^q , h_1^q is the only TMD PDF that survives the integration over transverse momentum. The transversity functions of the valence u and d quarks allow access to the nucleon tensor charge, a fundamental property of the nucleon that can also be calculated in lattice QCD [12,13]. The transversity PDF is chiral odd and thus not directly observable in inclusive DIS. In 1993, Collins suggested that it could be measured in SIDIS processes, where it appears coupled with another chiral-odd function [14], the so-called Collins fragmentation function $H_{1q}^{\perp h}$. The latter is the transverse-spin dependent fragmentation function (FF) that describes the correlation between the transverse spin of the quark q and the transverse momentum of the unpolarized final-state hadron h . This correlation leads to a left-right asymmetry in the distribution of hadrons produced in the fragmentation of transversely polarized quarks, which in SIDIS gives rise to a transverse-spin asymmetry, the so-called Collins asymmetry A_{Coll}^h . At leading order in perturbative QCD, this asymmetry is proportional to the convolution [11,15,16] of the transversity function and the Collins fragmentation function over transverse momenta. Independent essential information on $H_{1q}^{\perp h}$ is obtained from measurements of the e^+e^- annihilation process [17–21].

In SIDIS, the Collins effect produces a modulation $[1 + \epsilon_{\text{Coll}} \sin \phi_{\text{Coll}}]$ in the number of final state hadrons, where $\phi_{\text{Coll}} = \phi_h + \phi_s - \pi$ is the Collins angle, and ϕ_h and ϕ_s are the azimuthal angles of the hadron and of the target nucleon spin vector, respectively, in the reference system illustrated in Fig. 1. The amplitude of this modulation is $\epsilon_{\text{Coll}} = D_{\text{NN}} f P_t A_{\text{Coll}}^h$, where $D_{\text{NN}} \simeq (1 - y)/(1 - y + y^2/2)$ is the transverse-spin transfer coefficient from target quark to struck quark, y is the fractional energy of the virtual photon, f is the dilution factor of the target material, and P_t is the transverse polarization of the target nucleon.

The Sivers TMD PDF $f_{1T}^{\perp q}$ was introduced in 1990 [23] to explain the large transverse spin effects observed in $p\bar{p}$ collisions [24]. It describes the correlation of the intrinsic transverse momentum \mathbf{k}_T of the unpolarized quarks with the transverse spin of the nucleon. The final state interactions of the struck quark with the nucleon remnants lead

to a modulation of the type $[1 + \epsilon_{\text{Siv}} \sin \phi_{\text{Siv}}]$ in the distribution of the hadrons produced in SIDIS off transversely polarized nucleons. Here $\phi_{\text{Siv}} = \phi_h - \phi_s$ is the Sivers angle, and the amplitude of the modulation can be written as $\epsilon_{\text{Siv}} = f P_t A_{\text{Siv}}^h$, with A_{Siv}^h being the Sivers asymmetry (note that the Collins and Sivers asymmetries are denoted by $A_{\text{UT}}^{\sin(\phi_h + \phi_s - \pi)}$ and by $A_{\text{UT}}^{\sin(\phi_h - \phi_s)}$ in Ref. [25] and by $A_{\text{UT}}^{\sin \phi_{\text{Coll}}}$ and $A_{\text{UT}}^{\sin \phi_{\text{Siv}}}$ in Ref. [26]) that is proportional to the convolution of $f_{1T}^{\perp q}$ and the spin-averaged fragmentation function D_{1q}^h . Measuring azimuthal distributions of hadrons produced in SIDIS off a transversely polarized target allows the Collins and the Sivers effects to be disentangled [27]. The Collins and Sivers asymmetries are extracted from the same data, requiring measurements with proton and deuteron (or neutron) targets to allow for quark flavor separation.

The Collins and Sivers asymmetries were measured by the HERMES Collaboration at DESY scattering 27.6 GeV electrons on transversely polarized protons [6,7,28], by COMPASS with 160 GeV muons on transversely polarized deuterons (in the years 2002–2004) [8,9,29] and protons (in 2007 and 2010) [10,30,31], and by JLab with 5.9 GeV electrons on transversely polarized ^3He [32,33]. Clear signals of nonzero asymmetries were observed on protons, while the deuteron data and the ^3He data exhibited asymmetries compatible with zero, although with rather large statistical uncertainties. Extractions of Sivers and transversity functions from HERMES and COMPASS data, and e^+e^- Belle data [18] to constrain the Collins FF, were soon carried out by several groups [34–40], but the largely unbalanced statistics of the proton and deuteron data hampered an accurate extraction of the d -quark PDFs. Consequently, more deuteron data were mandatory. In 2022, the COMPASS Collaboration took SIDIS data using a transversely polarized ^6LiD target, with the primary goal of measuring the Collins and Sivers asymmetries with much higher precision. This dataset will remain unique until complementary measurements with transversely polarized nucleons are performed at JLab [41–43] and at the Electron Ion Collider [44].

The principle of the measurements, the COMPASS apparatus and the data analysis were already described in Refs. [30,31] and are only briefly summarized here for completeness. The spectrometer [45] was located in the CERN SPS North Area at the M2 beamline. In various configurations, COMPASS took data from 2002 to 2022. In order to combine large geometrical acceptance and wide kinematic coverage, the spectrometer consists of two magnetic stages. It comprises a variety of tracking detectors, a fast RICH, hadron and electromagnetic calorimeters, and provides muon identification via filtering through thick absorbers. The first stage uses a 1 Tm dipole magnet with an acceptance of about ± 200 mrad in both vertical and horizontal planes. The second stage uses a 4.4 Tm

spectrometer magnet, located 18 m downstream from the target, and the acceptance is ± 50 and ± 25 mrad in the horizontal and vertical plane, respectively. The detector components, the front-end electronics, the triggering system, the data acquisition and the data storage were designed to stand the associated rate of secondaries.

In 2022, the spectrometer configuration was very similar to that used in 2007 and 2010 [45], when SIDIS off transversely polarized protons was measured. In particular, the 180 mrad angular acceptance was significantly larger as compared to that of 70 mrad of the 2002–2004 measurements with the deuteron target.

The data were collected using a μ^+ beam with a nominal momentum of 160 GeV/c , as for all COMPASS measurements to study transverse-spin effects. The muons originated from the decay of π and K mesons produced by the 400 GeV SPS proton beam on a primary beryllium target and were naturally polarized by the weak decay mechanism. The beam polarization was about -80% and the momentum spread was $\Delta p/p = \pm 5\%$.

The target magnet can provide both a solenoid field up to 2.5 T and a dipole field up to 0.6 T. With such a configuration, the target polarization can be oriented either longitudinally or transversely to the beam direction. The target was cooled by a ${}^3\text{He}$ - ${}^4\text{He}$ dilution refrigerator, reaching ~ 50 mK in the frozen-spin mode. As for the previous measurement, ${}^6\text{LiD}$ was used as a deuteron target, since its favorable dilution factor (~ 0.4) and the high polarization achievable (~ 0.5) are of utmost importance. The target consisted of three cylindrical cells with a diameter of 3 cm, mounted coaxially to the beam. The central cell was 60 cm long, and the two outer ones were 30 cm long and 5 cm apart. Neighboring cells were polarized in opposite vertical directions, so that data for

both spin directions were recorded at the same time. The data taking was organized in periods, which were characterized by stable spectrometer performances. In the middle of each period, i.e., after three to six days, the spin orientation in the target was reversed to further minimize systematic effects.

In this Letter we present the analysis and the results from seven out of ten periods (corresponding to about two-thirds of the total statistics collected in 2022), for which data processing and systematic studies are completed. Candidate events are required to have reconstructed incoming and outgoing muons and reconstructed charged hadrons stemming from the muon interaction vertex. In order to ensure the DIS regime, only events with photon virtuality $Q^2 > 1 \text{ (GeV}/c)^2$, $0.1 < y < 0.9$, and mass of the hadronic final state system $W > 5 \text{ GeV}/c^2$ are considered. The hadrons are required to have a transverse momentum with respect to the virtual photon direction of $p_T > 0.1 \text{ GeV}/c$ and a fraction of the available energy of $z > 0.2$, leading to a total of about 40×10^6 positive hadrons and about 32×10^6 negative hadrons. Most of these hadrons are pions (about 70% for positive and 75% for negative hadrons), almost independent of the Bjorken variable x , of z and of p_T [46].

The asymmetries are measured separately for positive and negative hadrons as a function of x , z , or p_T . The binning is the same as used for the deuteron results from the 2002–2004 data [9] and the proton results from the 2007 and 2010 data [10,30,31]. In every bin of x , z or p_T , for each period the asymmetries are extracted from the number of hadrons produced in each cell for the two directions of the target polarization. Using an extended unbinned maximum likelihood estimator [10], all the 8 azimuthal modulations expected in the transverse spin-dependent part of the SIDIS cross section [11] are fitted simultaneously. In order to extract the Collins and Sivers asymmetries, the

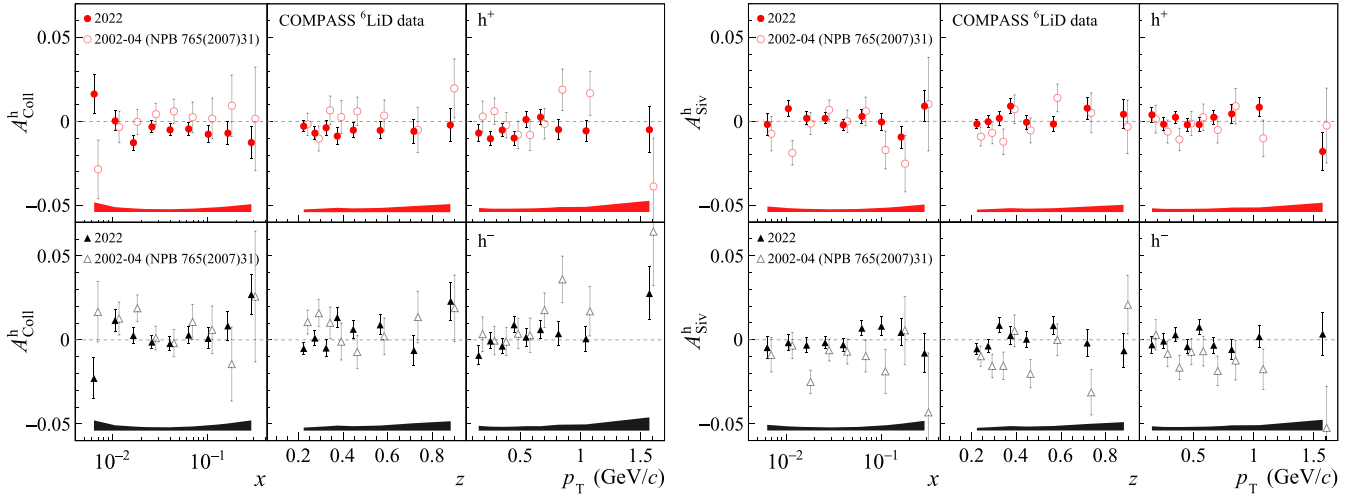


FIG. 2. Results for the Collins (top) and Sivers (bottom) asymmetries for deuterons from 2022 data as a function of x , z and p_T for positive (red circles) and negative (black triangles) hadrons. The error bars are statistical only. The bands show the systematic point-to-point uncertainties.

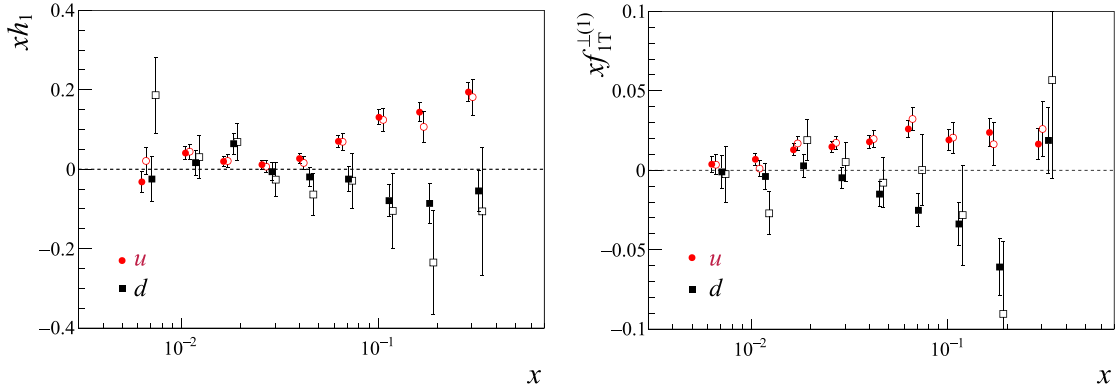


FIG. 3. Left: transversity functions for u -valence (red circles) and d -valence (black squares) quarks. The open points show the values obtained using the previously published results for the proton and deuteron Collins asymmetries. The filled points show the values obtained including the present deuteron results. The error bars show the statistical uncertainties. Right: the same for the first k_T^2 moments of the Sivers functions.

measured amplitudes of the modulations in $\sin \phi_{\text{Coll}}$ and $\sin \phi_{\text{Siv}}$ are divided by the mean values of the factors $D_{\text{NN}} f P_t$ and $f P_t$, respectively. The dilution factor of the ^6LiD material is calculated for semi-inclusive reactions as a function of x and y [47]; its mean value increases with x from 0.34 to 0.40, and it is $\simeq 0.38$ for all z and p_T bins. The values of the deuteron target polarization (about 0.4) are obtained from measurements, performed for each target cell and each period before and after repolarization and taking into account the relaxation time. The final asymmetries are obtained by averaging the results from the seven periods, after verifying their statistical compatibility.

As in the previous analyses [10,30], detailed studies were performed in order to quantify the systematic uncertainties. Various types of false asymmetries are measured from different combinations of the data, assuming a wrong direction of the target cell polarization. Differences between asymmetries extracted by splitting the data according to the reconstructed direction of the scattered muon in the spectrometer are also taken into account. The overall systematic point-to-point uncertainties are evaluated to be less than half of the statistical uncertainties. Systematic scale uncertainties are arising from the measurement of the target polarization (3%) and from the evaluation of the target dilution factor (2%).

Figure 2 shows A_{Coll}^h (top row) and A_{Siv}^h (bottom row) measured as a function of x , z , and p_T for positive and negative hadrons. The values are in good agreement with our previous measurements [8,9,29], with an important gain in precision: the statistical and the systematic uncertainties are reduced by up to a factor of 3. The present measurement of A_{Coll}^h indicates small negative (positive) signals for positive (negative) hadrons at large x , i.e., asymmetries with the same sign as those measured with the proton target. The Sivers asymmetries are again compatible with zero, despite the much smaller uncertainties. All numerical values are available on HEPData [48].

The present results are used together with the published proton [30,31] and deuteron [9] results of COMPASS to extract for u and d valence quarks the transversity distributions and the first k_T^2 moments of the Sivers functions. The latter are defined as $f_{1T}^{\perp(1)q}(x, Q^2) \equiv \int d^2k_T (k_T^2/2M^2) \times f_{1T}^{\perp q}(x, k_T^2, Q^2)$, with M being the proton mass (see, e.g., Ref. [40]).

The point-by-point extraction is performed by combining the proton and deuteron asymmetries in each x bin, following the simple and direct procedure of Refs. [36,49] and [40]. In each x bin the extraction is performed at the Q^2 value of the asymmetry measurement. Across the x bins, these values range from 1 to 50 $(\text{GeV}/c)^2$, with mean values between 1.3 and 23 $(\text{GeV}/c)^2$. In line with several phenomenological analyses, these extractions assume TMD factorization, a topic recently discussed in particular for unpolarized cross sections [50–52].

For the determination of the transversity distribution h_1 , the same Collins analysing power obtained from the Belle data [18] and the same spin-averaged PDFs and FFs as in Ref. [36] are used. The results for the u - and d -valence quark are shown in the left panel of Fig. 3. The open points are the values obtained using the previously published results for A_{Coll}^h and are the same as in Ref. [36], while the closed points are the values obtained using the weighted mean of the published and the present deuteron results. A considerable reduction of the uncertainties is observed in particular for $h_1^{d_v}$, reaching almost a factor of 4 in the last x bins. The good statistical balance between the present proton and deuteron data strongly reduces the statistical correlation between the extracted functions $h_1^{u_v}$ and $h_1^{d_v}$ in all x bins (correlation coefficient $0 < \rho < 0.1$). Table I shows that the new COMPASS measurement clearly improves the knowledge about the truncated tensor charges δu , δd and g_T , as obtained by integrating h_1 over the range

TABLE I. Truncated tensor charges δu , δd , and g_T in the range $0.008 < x < 0.210$ from numerical integration of the h_1 values, obtained using for A_{Coll}^h the previously published results only (first line) and adding the present results (second line).

Data	$\delta u = \int_{0.008}^{0.210} dx h_1^{u_v}(x)$	$\delta d = \int_{0.008}^{0.210} dx h_1^{d_v}(x)$	$g_T = \delta u - \delta d$
Previous [9,30,31]	0.187 ± 0.030	-0.178 ± 0.097	0.365 ± 0.078
Previous [9,30,31] and present	0.214 ± 0.020	-0.070 ± 0.043	0.284 ± 0.045

$0.008 < x < 0.210$ without correcting for the slow Q^2 evolution of h_1 in the range $1.5 < Q^2 < 10.5$ (GeV/c) 2 . For the u quark, new and old values are consistent, with a reduction of the statistical uncertainty by about 30% when adding the present results. For the d quark, the new values are a factor of about 2.5 smaller, with a reduction of the statistical uncertainty by a factor of 2. The sign and magnitude of δu and δd are in qualitative agreement with the lattice QCD calculations, although the values of h_1^u are smaller than those extracted in a recent phenomenological analysis that included more data and recent lattice results in the fit [53]. The isovector nucleon tensor charge g_T is now about 20% smaller, with the uncertainty reduced by almost a factor of 2.

The newly extracted values show that the transversity for the d quark is smaller in magnitude than that for the u quark, while still appearing to be opposite in sign. This is consistent with the case of the g_1^q helicity PDFs and with the fact that in the non-relativistic limit helicity and transversity are equal [54]. While h_1^d looks similar to g_1^d , in the case of the u quark the transversity PDF has smaller values and goes to zero at larger values of x , suggesting possible relativistic effects in the hadronic structure. Another relevant feature is that the new numerical values of h_1^d now lie within the so-called Soffer positivity bound [55].

For the Sivers function, we follow the procedure of Ref. [40] using the same spin-averaged PDFs and FFs and assuming that all charged hadrons are pions. The right panel of Fig. 3 shows the results for $f_{1T}^{\perp(1)u_v}$ and $f_{1T}^{\perp(1)d_v}$. The open points are the values obtained from the previously published A_{Siv}^h results only, while the filled ones are obtained adding the present deuteron results. For the d quark, the statistical uncertainties are reduced by about a factor of 2, and the values are now clearly negative in the range $0.04 < x < 0.21$. The values of $f_{1T}^{\perp(1)u}$ and $f_{1T}^{\perp(1)d}$ are in satisfactory agreement with recent phenomenological extractions (see, e.g., Ref. [56]) except for the region $x \simeq 0.02$ for the d quark, where $f_{1T}^{\perp(1)d}$ is very close to zero in our work.

In summary, this Letter presents the new high-statistics COMPASS results for the Collins and the Sivers asymmetries of charged hadrons measured from part of the SIDIS data collected in 2022 with a deuteron target. The asymmetries are given as a function of x , z , or p_T . They are

consistent with the previously published deuteron results, and the overall precision is improved by up to a factor of three. Combining the new deuteron data with all proton and deuteron data from COMPASS, both the transversity distribution and the first moments of the Sivers function are extracted. By numerically integrating the transversity distributions of the u and d valence quarks the tensor charge is evaluated in the range $0.008 < x < 0.21$. Altogether, the new COMPASS deuteron results are expected to have strong impact on the knowledge of the transverse-spin structure of the nucleon.

Acknowledgments—We acknowledge the support of the CERN management and staff, as well as the skills and efforts of the technicians of the collaborating institutes. In particular, we are grateful to the CERN Management and The Super Proton Synchrotron Experiments Committee (SPSC) for supporting the completion of COMPASS data taking with a full run in 2022. We thank Vincenzo Barone and Gunnar Schnell for useful discussions. This work was made possible by the financial support of our funding agencies: the Higher Education and Science Committee of the Republic of Armenia, in the frame of the research project No. 21AG-1C028 (Armenia); the MEYS Grants No. LM2023040, No. LM2018104 and No. LTT17018 (Czech Republic); the Charles University Grant No. PRIMUS/22/SCI/017 (Czech Republic); the BMBF Bundesministerium für Bildung und Forschung (Germany); the DFG cluster of excellence “Origin and Structure of the Universe” (Germany); the B. Sen fund (India); the Israel Academy of Sciences and Humanities; the Funds for Research 2019-22 of the University of Eastern Piedmont (Italy); the MEXT and JSPS under Grants No. 18002006, No. 20540299, No. 18540281 and No. 26247032 (Japan); the Daiko and Yamada Foundations (Japan); the NCN (Poland) Grant No. 2020/37/B/ST2/01547; the FCT Grants DOI 10.54499/CERN/FIS-PAR/0022/2019 and DOI 10.54499/CERN/FIS-PAR/0016/2021 (Portugal); the Ministry of Science and Technology (Taiwan); the National Science Foundation, Grant No. PHY-1506416 (USA); the European Union’s Horizon 2020 research and innovation programme under Grant Agreement STRONG—2020—No. 824093.

[1] G. Bunce *et al.*, *Phys. Rev. Lett.* **36**, 1113 (1976).
[2] G. L. Kane, J. Pumplin, and W. Repko, *Phys. Rev. Lett.* **41**, 1689 (1978).

[3] J. P. Ralston and D. E. Soper, *Nucl. Phys.* **B152**, 109 (1979).

[4] X. Artru and M. Mekhfi, *Z. Phys. C* **45**, 669 (1990).

[5] R. L. Jaffe and X. Ji, *Phys. Rev. Lett.* **67**, 552 (1991).

[6] A. Airapetian *et al.* (HERMES Collaboration), *Phys. Rev. Lett.* **94**, 012002 (2005).

[7] A. Airapetian *et al.* (HERMES Collaboration), *Phys. Rev. Lett.* **103**, 152002 (2009).

[8] V. Alexakhin *et al.* (COMPASS Collaboration), *Phys. Rev. Lett.* **94**, 202002 (2005).

[9] E. S. Ageev *et al.* (COMPASS Collaboration), *Nucl. Phys. B* **765**, 31 (2007).

[10] M. Alekseev *et al.* (COMPASS Collaboration), *Phys. Lett. B* **692**, 240 (2010).

[11] A. Bacchetta, M. Diehl, K. Goeke, A. Metz, P. J. Mulders, and M. Schlegel, *J. High Energy Phys.* 02 (2007) 093.

[12] J.-W. Chen, S. D. Cohen, X. Ji, H.-W. Lin, and J.-H. Zhang, *Nucl. Phys.* **B911**, 246 (2016).

[13] T. Bhattacharya, V. Cirigliano, S. D. Cohen, R. Gupta, H. W. Lin, and B. Yoon, *Phys. Rev. D* **94**, 054508 (2016).

[14] J. C. Collins, *Nucl. Phys.* **B396**, 161 (1993).

[15] A. Kotzinian, *Nucl. Phys.* **B441**, 234 (1995).

[16] P. J. Mulders and R. D. Tangerman, *Nucl. Phys.* **B461**, 197 (1996); **B484**, 538(E) (1997).

[17] K. Abe *et al.* (Belle Collaboration), *Phys. Rev. Lett.* **96**, 232002 (2006).

[18] R. Seidl *et al.* (Belle Collaboration), *Phys. Rev. D* **78**, 032011 (2008).

[19] J. P. Lees *et al.* (BABAR Collaboration), *Phys. Rev. D* **90**, 052003 (2014).

[20] J. P. Lees *et al.* (BABAR Collaboration), *Phys. Rev. D* **92**, 111101 (2015).

[21] M. Ablikim *et al.* (BESIII Collaboration), *Phys. Rev. Lett.* **116**, 042001 (2016).

[22] A. Bacchetta, U. D'Alesio, M. Diehl, and C. A. Miller, *Phys. Rev. D* **70**, 117504 (2004).

[23] D. W. Sivers, *Phys. Rev. D* **41**, 83 (1990).

[24] J. Antille, L. Dick, L. Madansky, D. Perret-Gallix, M. Werlen, A. Gonidec, K. Kuroda, and P. Kyberd, *Phys. Lett. 94B*, 523 (1980).

[25] C. Adolph *et al.* (COMPASS Collaboration), *Phys. Lett. B* **770**, 138 (2017).

[26] G. D. Alexeev *et al.* (COMPASS Collaboration), *Phys. Lett. B* **843**, 137950 (2023).

[27] D. Boer and P. J. Mulders, *Phys. Rev. D* **57**, 5780 (1998).

[28] A. Airapetian *et al.* (HERMES Collaboration), *Phys. Lett. B* **693**, 11 (2010).

[29] M. Alekseev *et al.* (COMPASS Collaboration), *Phys. Lett. B* **673**, 127 (2009).

[30] C. Adolph *et al.* (COMPASS Collaboration), *Phys. Lett. B* **717**, 376 (2012).

[31] C. Adolph *et al.* (COMPASS Collaboration), *Phys. Lett. B* **717**, 383 (2012).

[32] X. Qian *et al.* (Jefferson Lab Hall A Collaboration), *Phys. Rev. Lett.* **107**, 072003 (2011).

[33] Y. X. Zhao *et al.* (Jefferson Lab Hall A Collaboration), *Phys. Rev. C* **90**, 055201 (2014).

[34] M. Anselmino, M. Boglione, U. DAlesio, E. Leader, S. Melis, F. Murgia, and A. Prokudin, *Phys. Rev. D* **86**, 074032 (2012).

[35] M. Anselmino, M. Boglione, U. DAlesio, S. Melis, F. Murgia, and A. Prokudin, *Phys. Rev. D* **87**, 094019 (2013).

[36] A. Martin, F. Bradamante, and V. Barone, *Phys. Rev. D* **91**, 014034 (2015).

[37] Z.-B. Kang, A. Prokudin, P. Sun, and F. Yuan, *Phys. Rev. D* **93**, 014009 (2016).

[38] M. Anselmino, M. Boglione, U. DAlesio, J. O. Gonzalez Hernandez, S. Melis, F. Murgia, and A. Prokudin, *Phys. Rev. D* **92**, 114023 (2015).

[39] J. J. Ethier, N. Sato, and W. Melnitchouk, *Phys. Rev. Lett.* **119**, 132001 (2017).

[40] A. Martin, F. Bradamante, and V. Barone, *Phys. Rev. D* **95**, 094024 (2017).

[41] J. Arrington *et al.*, *Prog. Part. Nucl. Phys.* **127**, 103985 (2022).

[42] J. P. Chen, H. Gao, T. K. Hemmick, Z. E. Meziani, and P. A. Souder (SolID Collaboration), arXiv:1409.7741.

[43] A. Accardi *et al.*, arXiv:2306.09360.

[44] R. Abdul Khalek *et al.*, *Nucl. Phys.* **A1026**, 122447 (2022).

[45] P. Abbon *et al.* (COMPASS Collaboration), *Nucl. Instrum. Methods Phys. Res., Sect. A* **577**, 455 (2007).

[46] C. Adolph *et al.* (COMPASS Collaboration), *Phys. Lett. B* **744**, 250 (2015).

[47] E. S. Ageev *et al.* (COMPASS Collaboration), *Phys. Lett. B* **612**, 154 (2005).

[48] E. Maguire, L. Heinrich, and G. Watt, *J. Phys. Conf. Ser.* **898**, 102006 (2017).

[49] K. Augsten *et al.* (COMPASS Collaboration), Report No. SPSC-P-340-ADD-1, CERN-SPSC-2017-034, 2018.

[50] M. Boglione, A. Dotson, L. Gamberg, S. Gordon, J. O. Gonzalez-Hernandez, A. Prokudin, T. C. Rogers, and N. Sato, *J. High Energy Phys.* 10 (2019) 122.

[51] I. Scimemi and A. Vladimirov, *J. High Energy Phys.* **06** (2020) 137.

[52] A. Bacchetta, V. Bertone, C. Bissolotti, G. Bozzi, M. Cerutti, F. Piacenza, M. Radici, and A. Signori (MAP (Multi-dimensional Analyses of Partonic distributions) Collaboration), *J. High Energy Phys.* **10** (2022) 127.

[53] L. Gamberg, M. Malda, J. A. Miller, D. Pitonyak, A. Prokudin, and N. Sato (Jefferson Lab Angular Momentum (JAM) Collaboration), *Phys. Rev. D* **106**, 034014 (2022).

[54] R. Jaffe and X. Ji, *Nucl. Phys.* **B375**, 527 (1992).

[55] J. Soffer, *Phys. Rev. Lett.* **74**, 1292 (1995).

[56] A. Bacchetta, F. Delcarro, C. Pisano, and M. Radici, *Phys. Lett. B* **827**, 136961 (2022).